Research Article

Ta-Xi-San Suppresses Atopic Dermatitis Involved in Multitarget Mechanism Using Experimental and Network Pharmacology Analysis

Wenbing Zhi,[1] Chun Li,[2] Hong Zhang,[1,2] Yiding Zhao,[1] Shiyu Zong,[1] Qiqi Liu,[2] Jie Zhou,[2] Chunliu Wang,[1] Tingting Sun,[1] Yang Liu [iD],[1] and Ye Li [iD][1,2]

[1]*Shaanxi Academy of Traditional Chinese Medicine (Shaanxi Traditional Chinese Medicine Hospital), Xi'an 710003, China*
[2]*Pharmacy College, Shaanxi University of Chinese Medicine, Xianyang, Shaanxi, China*

Correspondence should be addressed to Yang Liu; liuyang311111@163.com and Ye Li; liyelsj@163.com

Atopic dermatitis (AD) is a relapsing and chronic skin inflammation with a common incidence worldwide. Ta-Xi-San (TXS) is a Chinese herbal formula usually used for atopic dermatitis in clinic; however, its active compounds and mechanisms of action are still unclear. Our study was designed to reveal the pharmacological activities, the active compounds, and the pharmacological mechanisms of TXS for atopic dermatitis. Mice were induced by 2,4-dinitrocluorobenzene (DNCB) to build atopic dermatitis model. The pathological evaluation, enzyme-linked immunosorbent assay (ELISA), and hematoxylin and eosin (H&E) assay were performed. The UPLC-Q-Exactive-MS^E and network pharmacology analysis were performed to explore active ingredients and therapeutic mechanisms of TXS. TXS treatment decreased levels of immunoglobulin E (IgE), interleukin-4 (IL-4), and tumor necrosis factor-α (TNF-α) in serum induced by DNCB. TXS reduced scratching behavior and alleviated inflammatory pathology of skin and ear. Meanwhile, TXS decreased the spleen index and increased spleen index. The UPLC-Q-Exactive-MS^E results showed that 65 compounds of TXS were detected and 337 targets were fished. We collected 1371 AD disease targets, and the compound-target gene network reveled that the top 3 active ingredients were (−)-epigallocatechin gallate, apigenin, and esculetin, and the core target genes were PTGS2, PTGS1, and HSP90AA1. The KEGG pathway and GO analysis showed that TXS remedied atopic dermatitis via PI3K-Akt signaling pathway, mitogen-activated protein kinase (MAPK) signaling pathway, and Toll-like receptor (TLR) signaling pathway with the regulation of inflammatory response and transcription. Further, we found that the targets of PTGS2 and HSP90AA1 were both elevated in ears and skin of AD model mouse; however, TXS decreased the elevated expressions of PTGS2 and HSP90AA1. Our study revealed that TXS ameliorated AD based on (−)-epigallocatechin gallate, apigenin, and esculetin via targeting PTGS2 and HSP90AA1.

1. Introduction

Atopic dermatitis (AD) is a relapsing, intensely pruritic inflammatory disordering of the skin [1]. It is one of the most common health problems and affects 2.1%–4.9% of human population worldwide [2]. Meanwhile, the morbidity of atopic dermatitis is high in both developing countries and developed countries [3, 4]. Atopic dermatitis is characterized by rash, erythema, edema, hemorrhage, lichenification, and severe itching, and it is always accompanied by destruction in skin barriers [5]. The pathogenesis of AD is closely related to the imbalance of T helper 2 (Th2) and T helper 1 (Th1)

factors [6]. Th2-based allergic inflammation plays a dominant role in the early stages of an acute outbreak of AD, which leads to the raised levels of IL-4, IL-13, and IgE [7]. However, Th1-dominant allergic inflammation is predominated in the chronic phase of AD and mainly releases IL-2, TNF-α, and IFN-γ [8, 9]. Moreover, multiple inflammatory cells are found in the epidermis and dermis of AD patients including mast cells, monocytes/macrophages, eosinophils, and T lymphocytes [10, 11].

Ta-Xi-San (TXS) is a Chinese herbal formula, consisting of six herbs: *Sophora flavescens* Aiton (*Kushen* in Chinese, KS)*, Phellodendron amurense* Rupr. (Huangbai in Chinese,

HB), *Sanguisorba* officinalis L. Bunge (*Diyu* in Chinese, DY), *Portulaca oleracea* L. (Machixian in Chinese, MCX), *Atractylodes lancea* (Thunb.) DC. (Cangzhu in Chinese, CZ), and Alumen (Baifan in Chinese, BF), which has widely used in the Shaanxi Traditional Chinese Medicine Hospital to treat skin swelling, itching, papules, and other dermatitis symptoms for nearly 15 years. The traditional uses of TXS consist of reducing heat and expelling toxins, expelling pus and dispersing swelling, and cooling the blood and hemostasis, all of which are associated with atopic dermatitis [12–15]. In the TXS prescription, the herb of *Sanguisorba* offcinalis L. has the ability to promote wound healing, relieve pains, and reduce inflammation reactions and tissue edema [16]. The herb *Phellodendron amurense* protects human keratinocytes from PM2.5-induced inflammation and contains the bioactive compounds for atopic dermatitis management [14, 17]. The herb *Phellodendron amurense* can reduce the skin swelling and ear tissue weight of the AD mouse induced by 2,4-dinitrochlorobenzene [18]. In addition, herb of *Sophora flavescens* presents effects of anti-inflammation and antioxidant [19, 20]. Moreover, multiple active constituents in these herbs are also exhibiting anti-inflammatory and antiallergic biological activities. Oxymatrine from *Sophora flavescens* was used for AD through increasing the IL-12 and IFN-γ mRNA levels and reducing the ICAM-1, MDC, and SOCS1 mRNA levels [21]. Gallic acid mitigated LPS-induced inflammatory response via suppressing NF-κB signaling pathway [22]. Atractylenolide I strongly inhibited 5-lipoxygenase to improve AD-like symptoms and decreased TNF-α, IL-6, and IL-1β production in lipopolysaccharide-induced acute lung jury [23, 24]. Berberine, as an index component of the *Phellodendron amurense*, suppressed the release of IL-6, CXCL8, and chemotactic factors in the eosinophils-dermal fibroblasts coculture [25]. However, the active constituents, molecular targets, and inherent pathways of TXS are rarely reported for AD treatment. Therefore, our study was designed for illustrating pharmacological effects and potential mechanisms.

Network pharmacology has made a significant contribution to systematically reveal the function and behavior between herbal formulas [26]. This research method systematically revealed effects and the potential mechanisms of multicomponent formula, through analyzing chemical component-target interaction networks [27]. Its dynamic and systematic characteristics are coincided with the theory of traditional Chinese medicine (TCM), which was suited for exploring the compound system of TCM with multiple components and multiple targets. The 63 constituents of the XIAOPI formula which prevents the breast cancer development were successfully found and validated based on network pharmacology [28]. Thus, we used AD mice model induced by DNCB to analyze efficacy of TXS and applied UPLC-Q-Exactive-Ms$^{\text{E}}$ and network pharmacology study to illuminate potential mechanism of TXS.

2. Materials and Methods

2.1. Materials and Reagents.
TXS was obtained from Shaanxi Academy of Traditional Chinese Medicine. Methanol and formic acid (LC-MS-grade) were purchased from Thermo Fisher Scientific Co., Ltd. (Waltham, MA, USA). 2,4-Dinitrofluorobenzene (DNCB) was purchased from Macklin Biochemical Technology Co., Ltd. Hydrocortisone Butyrate Cream was obtained from Hunan WZT Pharmaceutical Co., Ltd. (Xiangtan, China). The rat IL-4, TNF-α, and IgE ELISA kits were obtained from Nanjing Keygen Biotech (Nanjing, China). PTGS2 and HSP90AA1 ELISA kits were purchased from R&D (Minneapolis, MN, USA).

2.2. TXS Preparation.
TXS (160 g, Shaanxi Academy of Traditional Chinese Medicine) was soaked with 1000 mL in water for 30 min, decocted for 5 min again after boiled, and then filtrated. The decoction filtrated was concentrated to 160 mL (1 g crude drug/mL). The solution was filtered using 0.22 mm membranes. The filtrate was used and stored at 4°C before its use for animal assays.

2.3. Building Atopic Dermatitis Mice Model and Treatment.
BALB/c mice (male, 18–20 g) were purchased from Xi'an Jiao Tong University (Xian, China). All the mice were fed under the standard experimental conditions (-25 ± 2°C, humidity $60 \pm 5\%$, and 12/12 h day/night cycle). The AD mice model was induced by DNCB (dissolved in acetone/olive oil (3 : 1)), which was applied to dorsal skin and ear. Mice were segmented into 6 groups ($n = 6$ per group): (1) normal group, (2) matrix group, (3) DNCB model group, (4) DNCB + matrix + 0.65 mg crude drug/mL TXS, (5) DNCB + matrix + 1.30 mg crude drug/mL TXS, and (6) Hydrocortisone Butyrate Cream (Hyd B). Firstly, the mice were shaved with an aesthetic state (ethyl carbamate) using an electric shaver. Then, 100 μL 0.5% DNCB or acetone/olive oil (3 : 1) was applied to the shaved dorsal skin for 2 days, and there was no treatment in the 3rd~6th days . 70 μL 0.5% DNCB on dorsal skin and 20 μL 0.5% DNCB on ear every 2 days were applied from the 7th day. The AD model was finished on the 28th day for a total of 10 times (on days 1, 2, 7, 10, 13, 16, 19, 22, 25, and 28). DNCB was applied on the same site r. TXS was applied from the 7th day, 500 μL on dorsal skin and 200 μL on ears, twice a day until the 28th day. Hyd B was also applied from the 7th day, 300 mg on dorsal skin and 70 mg on ears, twice a day until the 28th day. The flowchart of the experimental program we studied is shown in Figure 1. Our animal study followed the guidelines (Care and Use of Laboratory in Xi'an Jiao Tong University Health Science Center, license approval no. SCXK (Shan) 2017-003).

2.4. Evaluation of Skin Lesion and Measurement of Ear Weight.
The relative severity of AD was evaluated weekly via scoring the lesions of the dermal tissues with the scoring procedure [29]: (1) erythema and hemorrhage, (2) erosion (excoriation), (3) edema, and (4) scaling (dryness). In each score, 0 was defined as exhibiting no symptoms, 1 as mild symptoms, 2 as moderate symptoms, and 3 as severe symptoms. Only one researcher participated in scoring the apparent AD symptoms throughout the experiment to
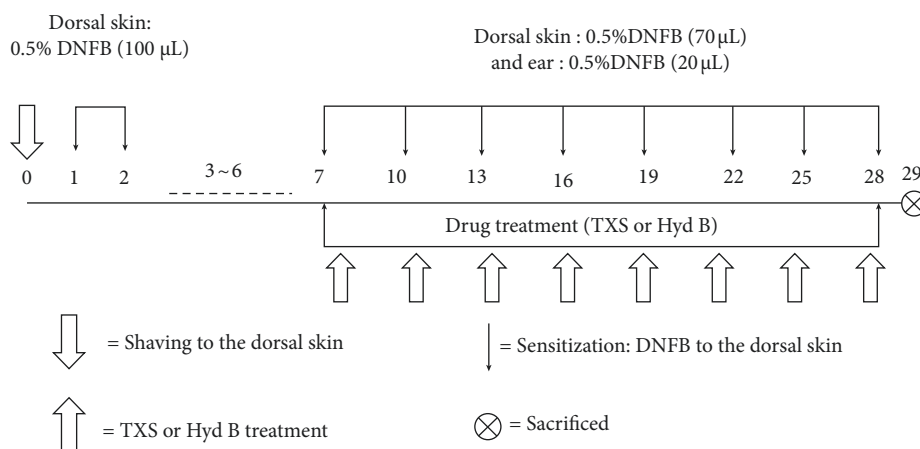
FIGURE 1: The schematic diagram of modeling method and treatment.

minimize technique variations. The ears of each mouse were harvested and weighted.

2.5. The Thymus Index and Spleen Index Measurement.

The spleen and thymus of mice in each group were removed integrally. The thymus index and spleen index were defined as the organ/body ratio (organ mass (mg)/corresponding animal mass (g)). The organ and the body weight were calculated using an electronic balance.

2.6. Histological Analysis.

The dorsal skin and ear samples were taken 24 h after final herbal administration and then fixed in 4% paraformaldehyde buffer, followed by embedding of the tissues in paraffin wax. The tissue sections were 2μm thick, and then they were stained with H&E.

2.7. Cytokines Quantitation.

Total IgE in serum was analyzed using an ELISA Quantitation Kit according to the manufacturer's protocol. The serum concentrations of the cytokines, including TNF-α and IL-4, were also quantified using a mouse cytokine enzyme immunoassay kit, respectively.

2.8. UPLC-Q-Exactive-MS^E Analysis.

The TXS aqueous extract was analyzed with a 150 mm × 2.1 mm Accucore AQ C18 column (2.6 μm). The mass spectrometer used in the UPLC-Q-Exactive-MS^E analysis was a quadrupole-electrostatic field orbital with an ESI mode and data treating used Mass Lynx 4.1 software. Column temperature was 30°C. The mobile phase consisted of 2 solvents: (A) 0.1% formic acid aqueous solution and (B) methyl alcohol (for a gradient elution program: 0–10 min, 95% solvent A; 20–30 min, 75% solvent A; 35 min, 30% solvent A; 45–60 min, 5% solvent A; 60–65 min, 95% solvent A). The flow rate was kept at 0.3 mL/ min. The injection volume was set as 1 μL. The ion source of thermoelectric spray (HESI) MS was performed to collect data in full switch ion mode. Other parameters were as follows: capillary temperature: 300°C, auxiliary gas heater: 300°C, sheath gas flow rate: 30 L/min, spray voltage: 3.50 kV,

full MS resolution: 7000, ddms2 resolution: 175000, and scan range: 100 to 1 200 Da. S-lens RF level was set as 55 V.

2.9. Network Pharmacology Study

2.9.1. Fishing Targets.

In this work, we search the targets of UPLC-Q-Exactive-MS^E analysis ingredients of TXS based on Traditional Chinese Medicine System Pharmacology Database and Analysis Platform (TCMSP, https://lsp.nwu.edu.cn/tcmsp.php) and the Comparative Toxicogenomics Database (CTD, https://ctd.mdibl.org/) based on UPLC-Q-Exactive-MS^E analysis. The UniProt (https://www.uniprot.org/) database was used for drug target revision to match the official name. The Online Mendelian Inheritance in Man (OMIM, https://www.omim.org/), Comparative Toxicogenomics Database (CTD, https://ctd.mdibl.org/) and GeneCards-Human Genes (GeneGards: https://www.genecards.org/) database were used to collect the AD-related disease genes.

2.9.2. Network Construction.

For better dissecting the latent active ingredients and key targets of TXS, we established the herb-ingredient-target-pathway network using Cytoscape 3.7.1 software. Then, the quantitative "degree" was analyzed by plugin network analyzer. According to the descending order of "degree," we selected the vital ingredients and targets of TXS against AD.

2.9.3. Functional Enrichment Assay.

The Gene Ontology (GO) enrichment and the Kyoto Encyclopedia of Genes and Genomes (KEGG) pathway (https://www.genome.jp/kegg/pathway.html) assay was performed based on the clusterProfiler software package on R platform and analyzed using visualization. Afterwards, the GO interactive network and the bubble diagram of KEGG pathway were structured using the top GO packet of R platform. $P < 0.05$ was calculated meaningfully in these two enrichment analyses.

2.10. Targets Verification.

To identify the targets of TXS on AD treatment, we performed the ELISA assay. The protein

Normal   Matrix   Model   TXS 0.65 mg/mL   TXS 1.3 mg/mL   Hyb B
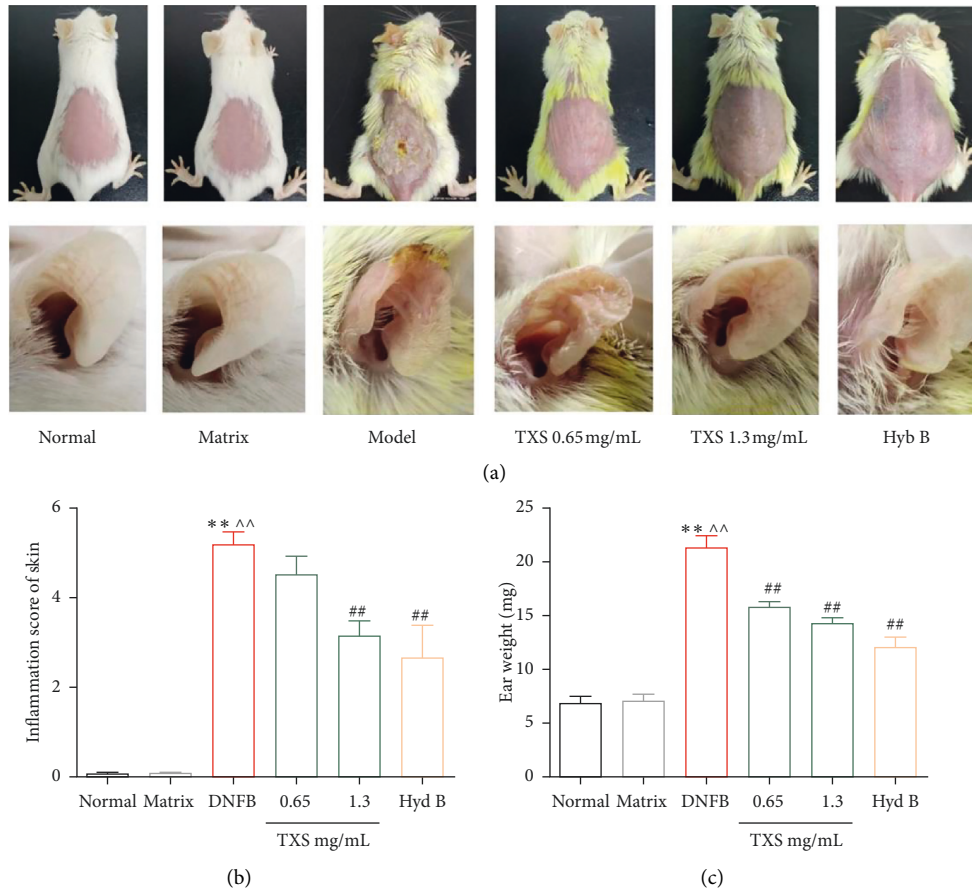
(a)

(b)

(c)

FIGURE 2: The morphological observation and assessment. (a) The morphological changes of skin and ears. (b) Inflammation score of skin. (c) The ear weight value. Values are expressed as mean ± SD ($n = 6$). * $P < 0.05$ and ** $P < 0.01$ compared with the normal group; $P < 0.05$ and $P < 0.01$ compared with the matrix group; #$P < 0.05$ and ##$P < 0.01$ compared with the DNFB model group.

expressions of PTGS2 and HSP90AA1 were quantitated. In brief, the ears and skin were fully ground with RIPA buffer adding 0.1 M PMSF and phosphatase inhibitors. Then, the supernatant was collected via centrifugation at 10000 rpm for 15 min at 4°C. The PTGS2 and HSP90AA1 expressions in supernatant were quantified using a mouse ELISA kit (R&D Systems, Minneapolis, MN, USA).

2.11. Statistical Analysis. Our data are shown as the mean ± standard deviation (SD). Statistical comparison among groups was analyzed with GraphPad Prism 5.01 (California, USA). ANOVA was firstly used followed by Student's *t*-test. $P < 0.05$ indicated significant difference between groups.

3. Result

3.1. TXS Alleviates the Lesions in Ear and Back. The skin inflammation of the back and ear of mice in each group was observed by visual method (Figure 2(a)). The skin of the ear and back of normal mice was smooth and healthy. Compared with the normal mice, the ear of mice in DNCB group was obviously swollen, rough, desquamate, and auricle with scab. Meanwhile, the back skin of mice in model group was

thickened, rough, erythema, desquamate, and scab, which showed a typical dermatitis feature. However, TXS dramatically decreased the excoriation, striking hemorrhage, and erosion and suppressed the scratching behavior compared to the DNCB-induced mice. In addition, in HYB treatment group, the inflammatory response was lighter, the damage and scratches just existed in edge of the ear, the back skin was thinner, and the vascular lines were clear.

At the same time, the lesion of back skin was scored according to the "inflammatory score standard." Compared with the normal mice, the back inflammatory score of mice in DNCB group was significantly enhanced, and TXS (1.3 mg crude drug/mL) significantly reduced the inflammatory score (Figure 2(b)). There was a significant increase in ear weight of mice in DNCB group due to swelling of the ear compared with the mice in the normal group (Figure 2(c)). TXS and HBY administration decreased the ear weight and back of mice, respectively. In conclusion, both TXS and HYB promoted inflammation subsidence and skin healing of mice.

3.2. TXS Improved the Thymus Index and Spleen Index. As Figures 3(a) and 3(b) show, compared with the normal group, the thymus index of mice in DNCB group was
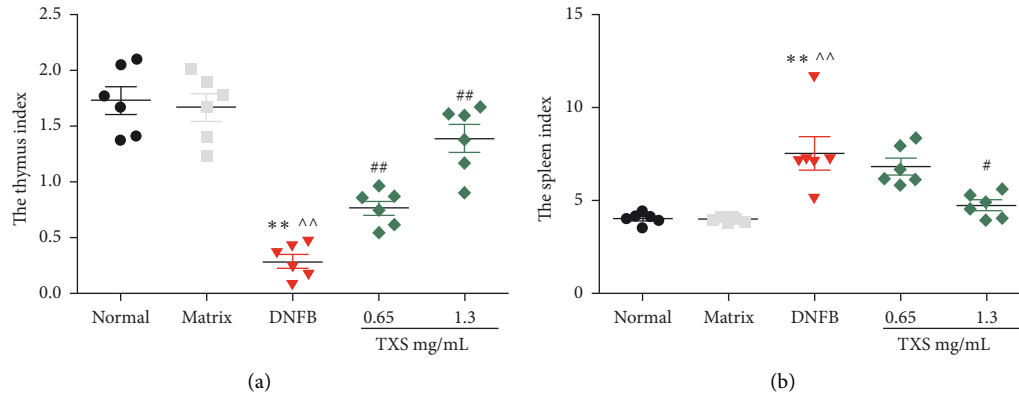
(a)

(b)

FIGURE 3: TXS regulates the thymus index and the spleen index. (a) The assessment of the thymus index. (b) The assessment of the spleen index. Values are expressed as mean ± SD ($n = 6$). * $P < 0.05$ and ** $P < 0.01$ compared with the normal group; ^ $P < 0.05$ and ^^ $P < 0.01$ compared with the matrix group; #$P < 0.05$ and ##$P < 0.01$ compared with the DNFB model group.

| Normal | Matrix | Model | TXS 0.65 mg/mL | TXS 1.3 mg/mL | Hyb B |

(a)

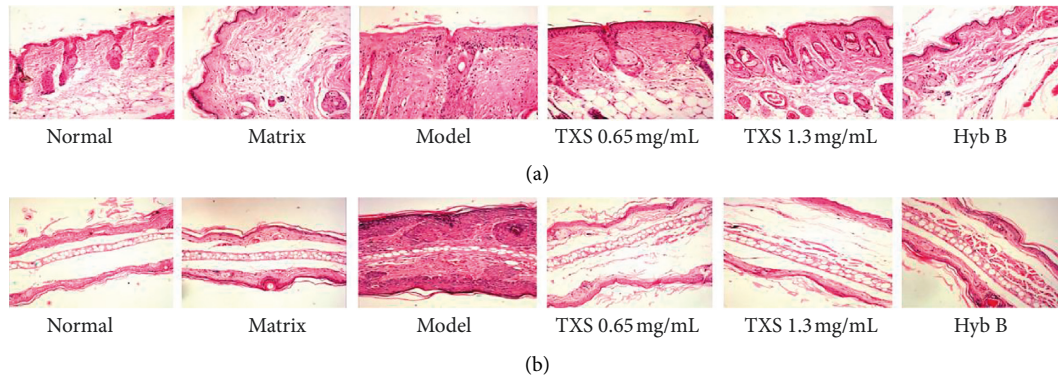| Normal | Matrix | Model | TXS 0.65 mg/mL | TXS 1.3 mg/mL | Hyb B |

(b)

FIGURE 4: TXS inhibits inflammation of skin and ears. ((a) and (b)) Hematoxylin and eosin- (H&E-) stained sections of skin tissues. Magnification x4.

memorably reduced; TXS administration could improve the thymus index of mice. The spleen index of DNCB-stimulated mice was significantly higher than that in the normal mice. High-dose TXS administration effectively reduced the spleen index.

3.3. Histological Analysis Results.
Hematoxylin study was used to recognize whether TXS regulates pathological symptoms of AD-like skin lesions and ear injury in DNFB-induced AD mouse model. In model group, skin tissues of mice showed typical inflammatory pathological changes including parakeratosis, thickening of the spinous layer, telangiectasia, and infiltration of inflammatory cells in the dermis (Figure 4(a)). In mice in TXS and HYB treatment group, there was no parakeratosis in skin tissue, and the spinous layer was thickened; however, a trifling infiltration of inflammatory cell was still in the dermis (Figure 4(a)). Meanwhile, ear histological analysis showed that TXS decreased the epidermal thickening and inflammatory cells accumulation in the lesions (Figure 4(b)).

3.4. TXS Regulated the Level of Cytokines.
Elevated levels of inflammatory cytokines and inflammatory cell infiltration

are a typical characteristic in AD [30]. Thus, we estimated the cytokines level in the serum of DNFB-sensitized mice. Subsequently, we observed that the TXS has an effect on the release of inflammatory factors. The levels of IL-4, TNF-α, and IgE in serum were significantly increased in the model group's mice induced by DNFB compared to the normal group. However, production of IL-4, TNF-α, and IgE was inhibited by TXS and Hyd B treatment (Figures 5(a)–5(c)).

3.5. The Ingredients Analysis of TXS Extracts.
The herb components of TXS extracts were detected via aligning each detectable compound mass data for each detectable compound with structure and confirmed by MS^E substructure data. The Base Peak Chromatogram (BPC) of TXS extracts in positive ion mode and negative ion mode is shown in Figures 6(a) and 6(b). TXS mainly contained alkaloids and flavonoid glycosides, and these ingredients presented a better MS response in positive than in the positive ion mode. In this research, 65 compounds extracted in TXS were identified through comparing and analyzing the primary and secondary mass spectrometry information, combining with databases (Metlin, Massbank, and Human Metabolome Database) and combining with retention behavior, database,
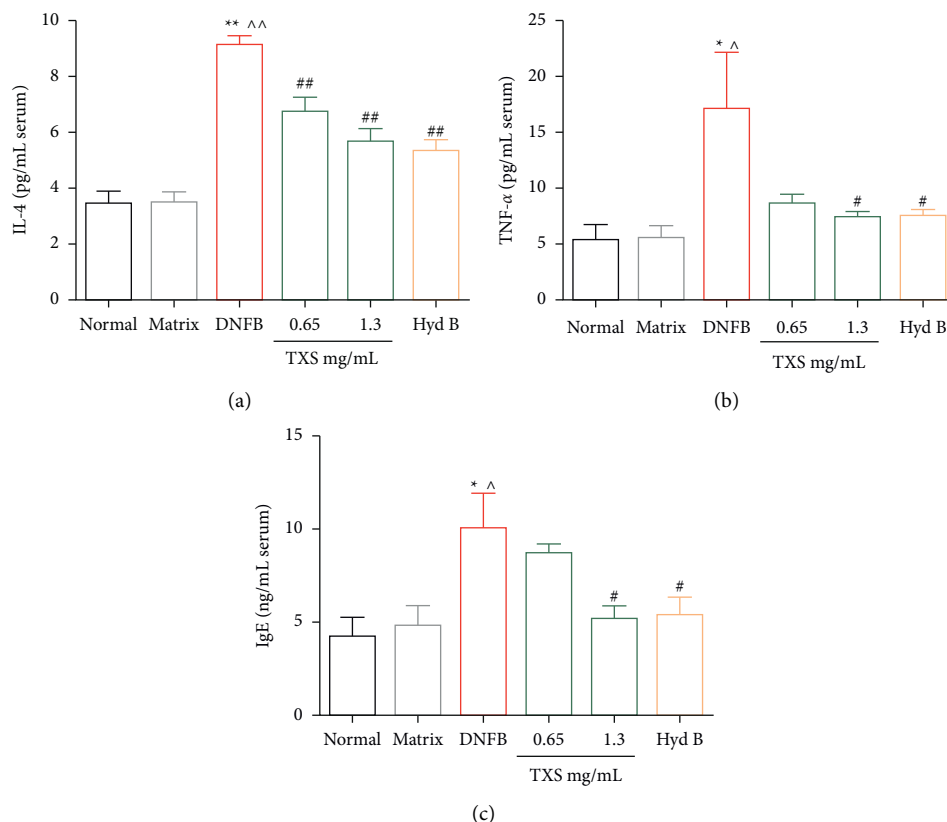
(a)

(b)

(c)

Figure 5: TXS decreases cytokines in serum. (a) The level of IL-4 in serum was determined by ELISA. (b) The level of TNF-α in serum was determined by ELISA. (c) The IgE production in serum was calculated by ELISA. Values are expressed as mean ± SD ($n = 6$). * $P < 0.05$ and ** $P < 0.01$ compared with the normal group; ˆ$P < 0.05$ and ˆˆ$P < 0.01$ compared with the matrix group; #$P < 0.05$ and ##$P < 0.01$ compared with the DNFB model group.

and related literature reports. The 65 compounds were confirmed as the principal compounds for the following assay and are detailedly displayed in Table 1.

3.6. Potential Target Genes and Network Analysis.
The 337 targets were collected form the 65 compounds in TXS based on UPLC-Q-Exactive-MS^E analysis after eliminating the duplicate targets. Simultaneously, 1371 AD-related targets were collected via searching CTD, GeneCards, and OMIM databases, and 1241 targets were decontaminated after removing duplicates. Then the compound targets and disease-related targets were merged, and we got the compound-target gene network.

The ingredient-target gene network is presented in Figure 7. This network consisted of 190 nodes (1 TXS formula node, 52 compounds, and 137 target genes) and 522 edges. Compounds in the network were classified as catechin class, flavonoids, coumarin, isoflavone, and alkaloids. Particularly, as shown in Tables 2 and 3, the top five ingredients of TXS which have maximum degrees are (−)-epigallocatechin gallate, apigenin, esculetin, wogonin, and epicatechin. Additionally, 27 genes (ADH1C, ADRA1B, IL-4, RELA, TP53, TOP2A, TNF, RXRA, PTGS2, PTGS1, PRKACA, PPARG, PIK3CG, NOS3, NOS2, NFKBIA, MAOA, JUN, HSP90AA1, ESR1, CDKN1A, CCND1, CASP3, BCL2, AR, AKT1, and ADRB2) were recognized due

to their interactions with more than five ingredients. The ingredient-target gene network contributed to understanding the possible effects of TXS.

3.7. The Results of KEGG and GO Analysis.
KEGG pathway enrichment showed that 199 pathways were harvested and the remarkable 30 related pathways are presented in Figure 8(a). Pathways in PI3K-Akt signaling pathway, MAPK signaling pathway, and TNF signaling pathway may be the latent mechanism to exert effects of TXS against AD. Subsequently, the results of GO evaluation of the top 10 enriched results are shown in Figure 8(b). The enriched biological process ontologies were dominated by positive regulation of transcription from RNA polymerase II promoter, negative regulation of apoptotic process, response to drug, inflammatory response, and positive regulation of transcription. The molecular function of targets was mainly enriched in ontologies including protein binding, identical protein binding, protein homodimerization activity, and enzyme binding. Meanwhile, cell component result showed that cytoplasm is the largest constitution.

3.8. TXS Regulated the PTGS2 and HSP90AA1 Expressions in Mouse Model.
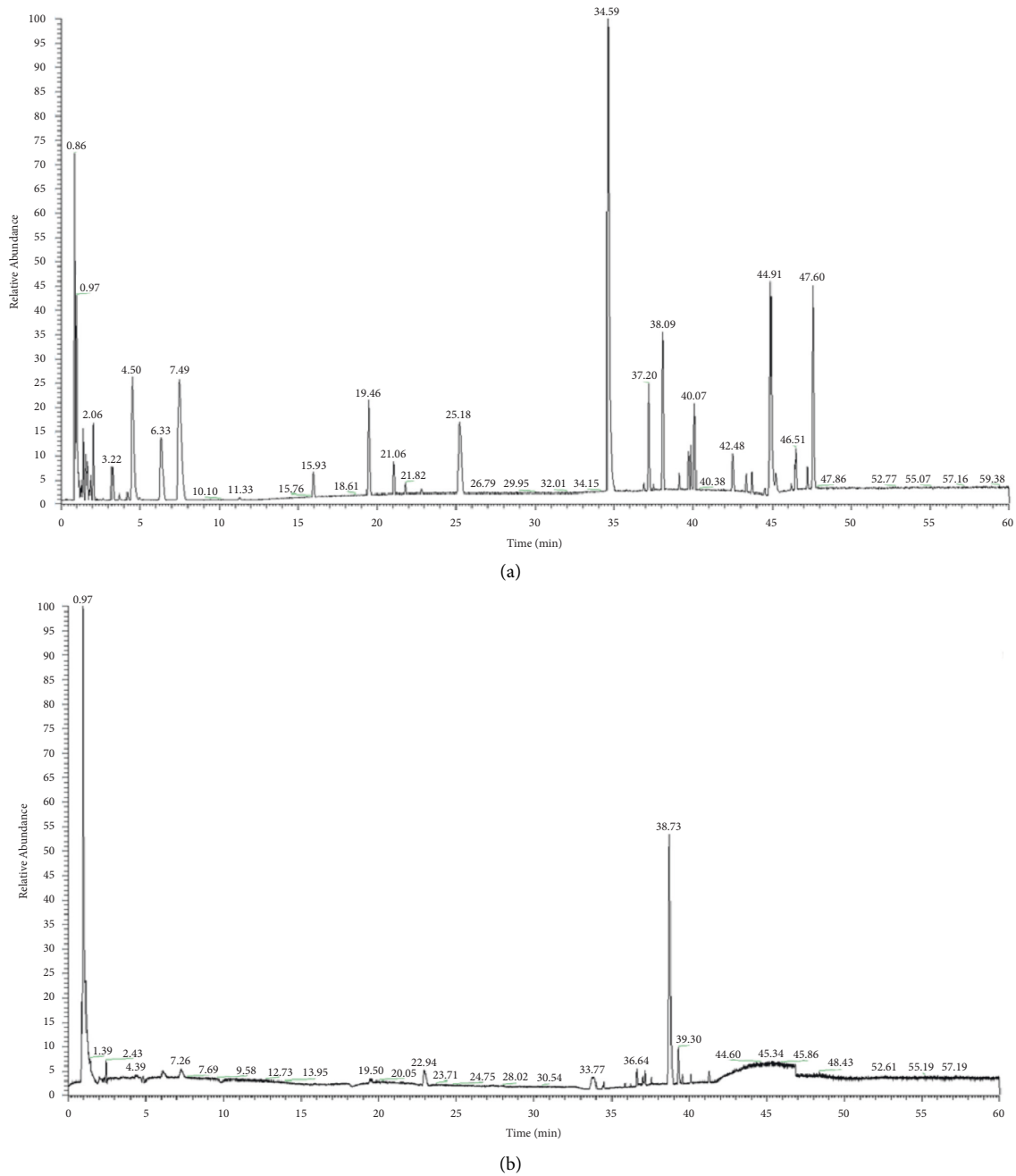PTGS2 and HSP90AA1 are major

FIGURE 6: The detection of chemical components in TXS. (a) UPLC-Q-Exactive-MS^E total ion current chromatogram of TXS under positive ion mode. (b) UPLC-Q-Exactive-MS^E total ion current chromatogram of TXS under negative ion mode.

regulatory targets for inflammatory response in AD and are core targets screened via network pharmacology. Thus, we investigate the regulatory effect of TXS on activation of PTGS2 and HSP90AA1. In our study, we found that the protein expressions of PTGS2 and HSP90AA1 in ears and skin of model mice were significantly enhanced compared to the normal mice; however, TXS decreased the elevated expressions of PTGS2 and HSP90AA1 (Figures 9(a)–9(d)). Our results revealed that TSX might be a useful drug for AD therapy via regulating PTGS2 and HSP90AA1 expressions.

4. Discussion

The DNCB-induced skin lesion in mice is a classical animal model for AD research [31]. Thus, we established DNCB-induced mouse model to assess the effects of TXS on AD. IL-4 and TNF-α are risk factors for developing atopic dermatitis [32]. Previous studies showed that cytokines including IL-4, TNF-α, and IL-1β-were enhanced in serum of AD patients [33]. Higher level of IFN-γ and IL-6 was detected in skin lesions of AD patients [34]. In our study, the levels of IL-4, TNF-α, INF-γ, and IgE in serum were reduced; meanwhile,

TABLE 1: The chemical composition analysis of TXS decoction by UPLC-Q-Exactive-MS^E

No.	Compound	Area	RT (means)	Formula	Measure m/z	Fragmentation	Delta m/z	Adducts	±	Sources
1	Matrine	1980000000	4.42	$C_{15}H_{24}N_2O$	249.2	70.065, 84.0868, 152.1433	−2.46	H		KS
2	Oxysophocarpine	1200000000	6.22	$C_{15}H_{22}N_2O_2$	263.18	—	−1.68	H	+	KS
3	7-Demethylsuberosin	139000	36.68	$C_{14}H_{14}O_3$	253.08	55.0545, 69.0699, 83.0854	−4.13	Na	+	KS
4	Kurarinone	948000	38.38	$C_{26}H_{30}O_6$	461.19	—	−1.54	Na	+	KS
5	Kushenol F	939000	39.72	$C_{25}H_{28}O_6$	423.18	—	0.13	H	−	KS
6	Trifolirhizin	118000000	36.85	$C_{22}H_{22}O_{10}$	469.11	149.0228, 193.0491, 237.0754	−1.2	Na	+	KS
7	Xanthohumol	836000	37.48	$C_{21}H_{22}O_5$	353.14	112.9856, 129.9757, 248.9604	−0.13	Na	−	KS
8	Isoxanthohumol	3600000	37.49	$C_{21}H_{22}O_5$	377.14	92.5511, 192.9041, 203.1646	−1.33	Na	+	KS
9	Oxymatrine	2.87E + 09	7.38	$C_{15}H_{24}N_2O_2$	265.19	136.112, 205.1333, 247.1802	−2.45	H	+	KS
10	Methylparaben	354000000	1.53	$C_{12}H_{16}N_2O$	205.13	58.0653, 91.0539, 146.0602	−1.84	H	+	KS
11	Formononetin	5670000	37.05	$C_{16}H_{12}O_4$	291.06	\	−1.7	H	+	KS
12	Sophocarpine	370000000	7.42	$C_{15}H_{22}N_2O$	247.18	98.0599, 150.1276, 148.1118	−1.58	H	+	KS
13	Neochlorogenic acid	5300000	18.35	$C_{16}H_{18}O_9$	355.1	92.5453, 120.9673, 142.9385	−1.82	H	+	HB
14	Palmatine	80100000	34.85	$C_{21}H_{22}NO_4$	352.15	127.1117, 327.2526, 377.2648	−1.91	H	+	HB
15	Oxyberberine	25000000	27.16	$C_{20}H_{17}NO_5$	352.12	62.1674, 79.1569, 138.1779	−1.73	H	+	HB
16	Tetrahydropalmatine	60200000	22.48	$C_{21}H_{25}NO_4$	356.19	149.012, 167.0225, 315.1926	−1.35	H	+	HB
17	Rutaevin	3940000	16.31	$C_{26}H_{30}O_9$	504.22	116.9857, 134.9963, 164.9843	−1.33	NH4	+	HB
18	Epiberberine	6320000000	34.6	$C_{20}H_{18}NO_4$	337.12	149.012, 167.0225, 307.1769	−2.58	H	+	HB
19	Phellodendrine	1210000000	44.75	$C_{20}H_{24}NO_4$	343.17	66.6729, 84.9595, 126.2253	−2.31	H	+	HB
20	Berberine	6320000000	39.32	$C_{20}H_{18}NO_4$	337.12	79.9573, 96.96, 309.1704	−2.58	H	+	HB
21	Coniferin	5470000	16.79	$C_{16}H_{22}O_8$	365.12	116.9857, 149.012, 164.9843	−1.49	H	+	HB
22	Vanillin	9890000	18.37	$C_8H_8O_3$	153.05	105.0031, 116.9857, 149.0119	−0.56	H	+	HB
23	Paeonol	35700000	38.34	$C_9H_{10}O_3$	167.07	56.965, 116.9857, 167.0025	−0.84	H	+	HB
24	Isovanillin	9890000	18.37	$C_8H_8O_3$	153.05	—	−0.56	H	+	HB
25	Berberrubine	17900000	33.67	$C_{19}H_{15}NO_4$	322.11	79.9055, 242.4609, 269.4887	−1.39	H	+	HB
26	Ethyl caffeate	1990000	22.86	$C_{11}H_{12}O_4$	209.08	72.0835, 80.518, 105.3846	1.68	H	+	HB
27	Limonin	101000000	35.78	$C_{26}H_{30}O_8$	493.18	88.3646, 250.7163, 350.8599	−1.86	H	+	HB/CZ
28	Ferulic acid	387000	40.09	$C_{10}H_{10}O_4$	195.07	65.0387, 95.049, 121.0282	−0.41	H	+	HB
29	Esculetin	1570000	16.43	$C_9H_6O_4$	177.02	58.9718, 90.998, 94.993	−0.24	H	−	HB
30	L-Adenosine	39200000	2.22	$C_{10}H_{13}N_5O_4$	268.1	94.0397, 119.0351, 136.0617	−1.8	H	+	HB
31	Tetrahydroberberine THB	1930000	21.77	$C_{20}H_{21}O_4N$	340.15	64.0373, 142.9384	−1.17	H	+	HB
32	Berbamine	295000	36	$C_{37}H_{40}N_2O_6$	609.29	—	−2.32	H	+	HB
33	Jatrorrhizine	347000	42.29	$C_{20}H_{20}NO_4$	339.15	64.0373, 142.9384	0.55	H	+	HB

TABLE 1: Continued.

No.	Compound	Area	RT (means)	Formula	Measure m/z	Fragmentation	Delta m/z	Adducts	±	Sources
34	Gallic acid	139000000	2.45	$C_7H_6O_5$	169.01	69.0345, 97.0294, 125.0249	−0.98	H	−	DY
35	Gallic acid trimethyl ether	2260000	31.94	$C_{10}H_{12}O_5$	213.08	—	−1.1	H	+	DY
36	(−)-Epigallocatechin gallate	277000	21	$C_{22}H_{18}O_{11}$	457.08	—	−1.45	H	−	DY
37	Epigallocatechin	4470000	1.53	$C_{15}H_{14}O_7$	307.08	93.8318, 122.1348, 174.7394	4.4	H	+	DY
38	Brevifolincarboxylic acid	446000	20.04	$C_{13}H_8O_8$	315.01	106.3279, 210.9946, 310.6447	−1.36	Na	+	DY
39	(−)-Epicatechin gallate	6400000	1	$C_{22}H_{18}O_{10}$	441.08	79.9573, 94.9808, 96.96	−1.01	H	−	DY
40	Epicatechin	80300000	15.85	$C_{15}H_{14}O_6$	289.07	97.0294, 109.0294, 123.0451	−0.57	H	−	DY
41	Protocatechuic acid	2660000	4.88	$C_7H_6O_4$	153.02	—	−0.58	H	−	DY
42	Methyl gallate	2920000	8.55	$C_8H_8O_5$	183.03	79.9573, 95.9522, 118.9419	−0.71	H	−	DY
43	Procyanidin B1	16600000	14.89	$C_{30}H_{26}O_{12}$	577.14	55.9346, 72.937, 90.9476	−0.24	H	−	DY
44	Procyanidin B2	16600000	14.89	$C_{30}H_{26}O_{12}$	577.14	55.9346, 72.937, 90.9476	−0.24	H	−	DY
45	Ethyl gallate	13400000	21.71	$C_9H_{10}O_5$	197.05	96.9601, 128.0352, 152.895	−0.25	H	−	DY
46	Ellagic acid	1020000	34.79	$C_{14}H_6O_8$	301	—	0.52	H	−	DY
47	Hyperoside	308000	40.62	$C_{21}H_{20}O_{12}$	465.1	—	0.86	H	+	DY
48	Ursonic acid	26600000	37.47	$C_{30}H_{46}O_3$	455.35	107.9667, 192.0492, 236.9945	−1.03	H	+	DY
49	Cianidanol	80300000	15.85	$C_{15}H_{14}O_6$	289.07	97.0294, 109.0294, 123.0451	−0.57	H	−	DY
50	Atractylodin	16400000	37.6	$C_{13}H_{10}O$	183.08	91.0541, 95.0490, 119.0490	−0.89	H	+	CZ
51	Atractylenolide II	40400000	38.09	$C_{15}H_{20}O_2$	255.14	55.0545, 69.0699, 83.0854	−1.4	Na	+	CZ
52	Atractylenolide I	2150000	37.76	$C_{15}H_{18}O_2$	254.12	55.0545, 69.0699, 81.0197	−0.09	H	+	CZ
53	Wogonin	11500000	35.27	$C_{16}H_{12}O_5$	285.08	—	−1.41	H	+	CZ
54	Baicalin methyl ester	4180000	36.9	$C_{22}H_{20}O_{11}$	283.09	—	−1.19	Na	+	CZ
55	Atractyloside A	27400000	36.27	$C_{21}H_{36}O_{10}$	471.22	64.023, 190.5318, 350.8599	−1.57	Na	+	CZ
56	Vanillic acid	488000	1.01	$C_8H_8O_4$	169.05	59.965, 57.935, 84.9586	−1.59	H	+	CZ
57	Protocatechualdehyde	3620000	37.47	$C_7H_6O_3$	139.04	72.9370, 97.0074, 111.0231	−0.43	H	+	CZ
58	Citric acid	327000000	0.96	$C_6H_8O_7$	191.02	85.0295, 87.0086, 111.0087	−0.4	H	−	MCX
59	Benzoic acid	82900000	1.75	$C_7H_6O_2$	123.04	65.0386, 77.0384, 95.0490	−1.49	H	+	MCX
60	Caffeic acid	23200000	40.11	$C_9H_8O_4$	181.05	95.0490, 103.0540, 121.0646	−1.32	H	+	MCX
61	Apigenin	2230000	36.31	$C_{15}H_{10}O_5$	269.05	—	0.05	H	−	MCX/ KS
62	Allantoin	2830000	0.99	$C_4H_6N_4O_3$	159.05	57.0700, 91.0541, 115.0546	−0.96	H	+	MCX
63	Isoscopoletin	3950000	37.01	$C_{10}H_8O_4$	193.05	133.052, 148.0755, 191.1195	−0.76	H	+	MCX
64	Mannitol	14000000	0.97	$C_6H_{14}O_6$	205.07	56.0497, 58.0653,146.0602	−2.05	H	+	MCX
65	Scopolin	24500000	18.28	$C_{16}H_{18}O_9$	377.08	92.5511, 129.6406, 203.1646	−1.57	H	+	MCX

Note: KS stands for *Sophora flavescens*; HB stands for *Phellodendron amurense*; DY stands for *Sanguisorba officinalis* L.; CZ stands for *Atractylodes lancea*; MCX stands for *Portulaca oleracea*.
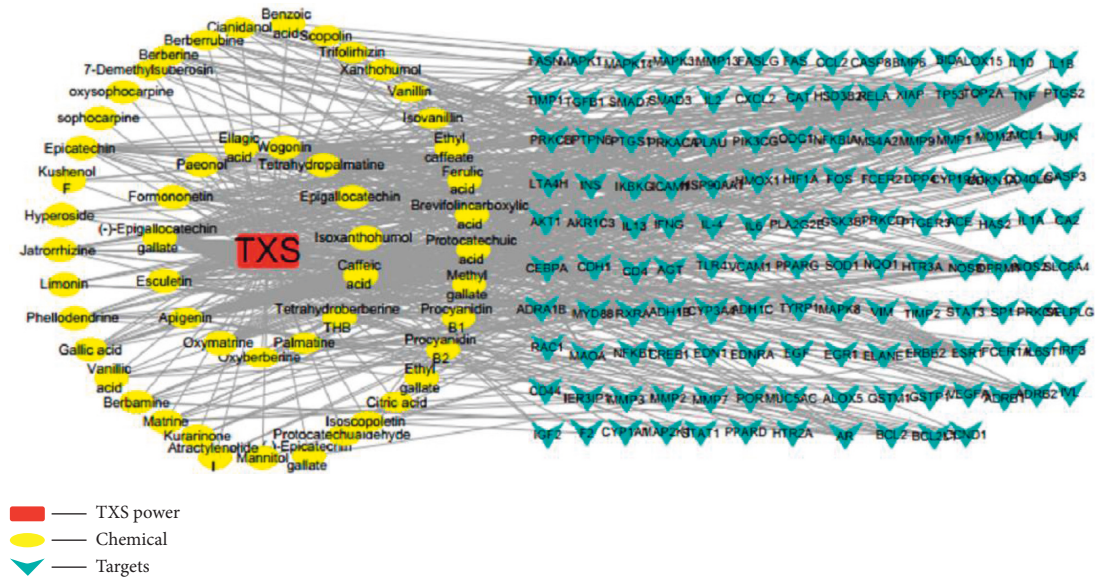
FIGURE 7: The component-targets network of TXS against AD.

TABLE 2: The pharmacodynamic compounds of TXS for AD.

No.	Compound	Betweenness centrality (BC)	Closeness centrality (CC)	Degree
1	(−)-Epigallocatechin gallate	0.3317	0.4797	61
2	Apigenin	0.1750	0.4355	41
3	Esculetin	0.1296	0.4219	34
4	Wogonin	0.0668	0.4127	29
5	Epicatechin	0.0483	0.3954	19
6	Formononetin	0.0371	0.39375	18
7	Oxymatrine	0.0714	0.3889	15
8	Ellagic acid	0.0459	0.3873	14
9	Paeonol	0.0200	0.3873	14
10	Caffeic acid	0.0457	0.3857	13

TABLE 3: The pharmacodynamic targets of TXS for AD.

No.	Target	Betweenness centrality (BC)	Closeness centrality (CC)	Degree
1	PTGS2	0.12968939	0.48461538	41
2	PTGS1	0.03576985	0.38729508	27
3	HSP90AA1	0.02247622	0.36914063	21
4	ESR1	0.0193549	0.38259109	15
5	PRKACA	0.00849434	0.34615385	14
6	RXRA	0.00732045	0.32926829	14
7	NOS2	0.01528486	0.37951807	12
8	ADRB2	0.00526221	0.32363014	11
9	TNF	0.03753438	0.42376682	11
10	TOP2A	0.00637523	0.33392226	11

the inflammation of back skin, the skin inflammation score, and the ear swelling of mice were alleviated after taking the TXS. Hence, TXS might be effective to balance atopic and inflammatory disorders in the progress of atopic dermatitis.

In addition, to explore the effects of TXS on skin and ear inflammation, we performed H&E assay and examined thymus index and spleen index. The mice induced by DNFB showed typical AD features, such as epidermal hyperplasia and massive inflammatory cells infiltration, which were coincided with the typical symptoms of AD. TXS treatment

effectively improved the skin and ear status. The thymus is a major immune organ, the index of which is an important index for assessing immunity [35]. Meanwhile, as another lymphatic organ of the human body, the spleen palys a core role in immune system and is used for assessing immuno-modulatory effects of drugs [36]. TXS treatment lowered the spleen index and enhanced the thymus index. Therefore, TXS regulated pathological changes in the development of AD.

UPLC-Q-Exactive-MS^E as a rapid, efficient, and sensitive method is always used for analyzing extracts and bioactive
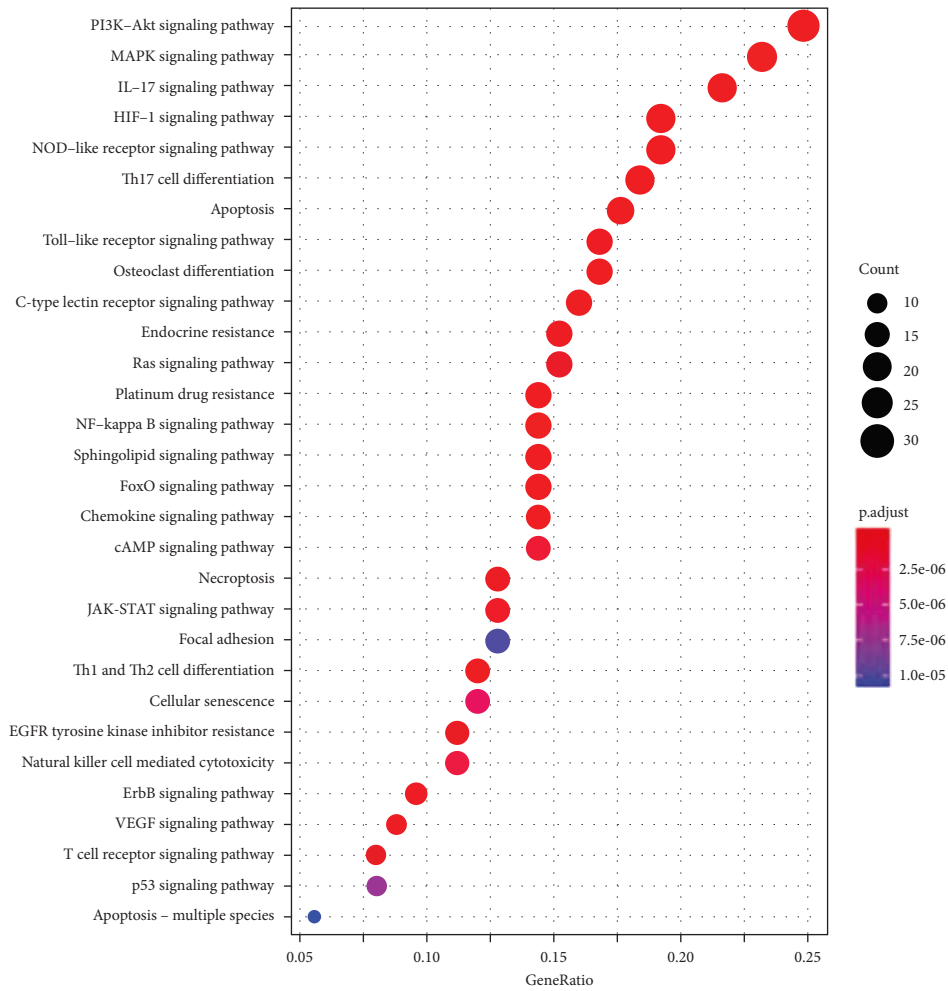
(a)
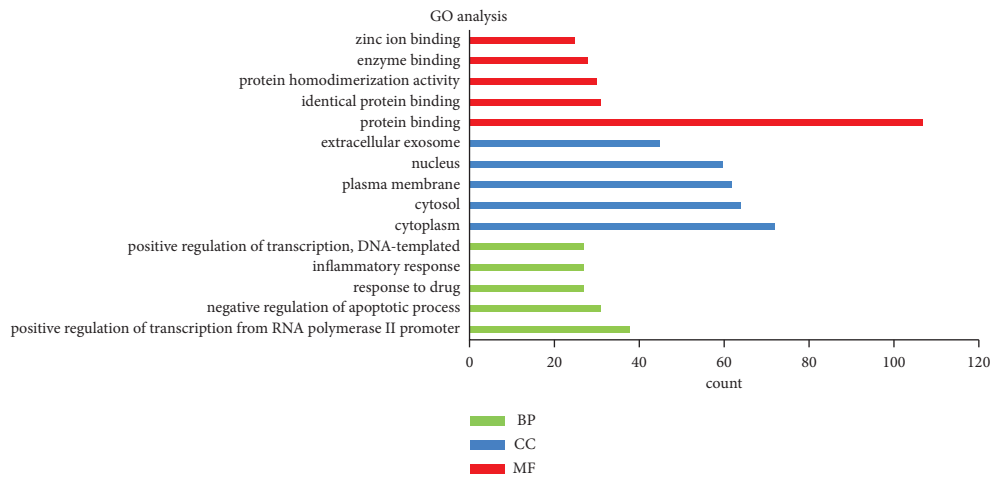
(b)

FIGURE 8: The mechanism exploration of TXS against AD. (a) KEGG pathway enrichment analysis of the TXS predicted targets. Bubble diagram of the top 30 KEGG pathways. (b) The top 5 GO analysis terms for CC, BP, and CF with the most significant P values of targets in AD.
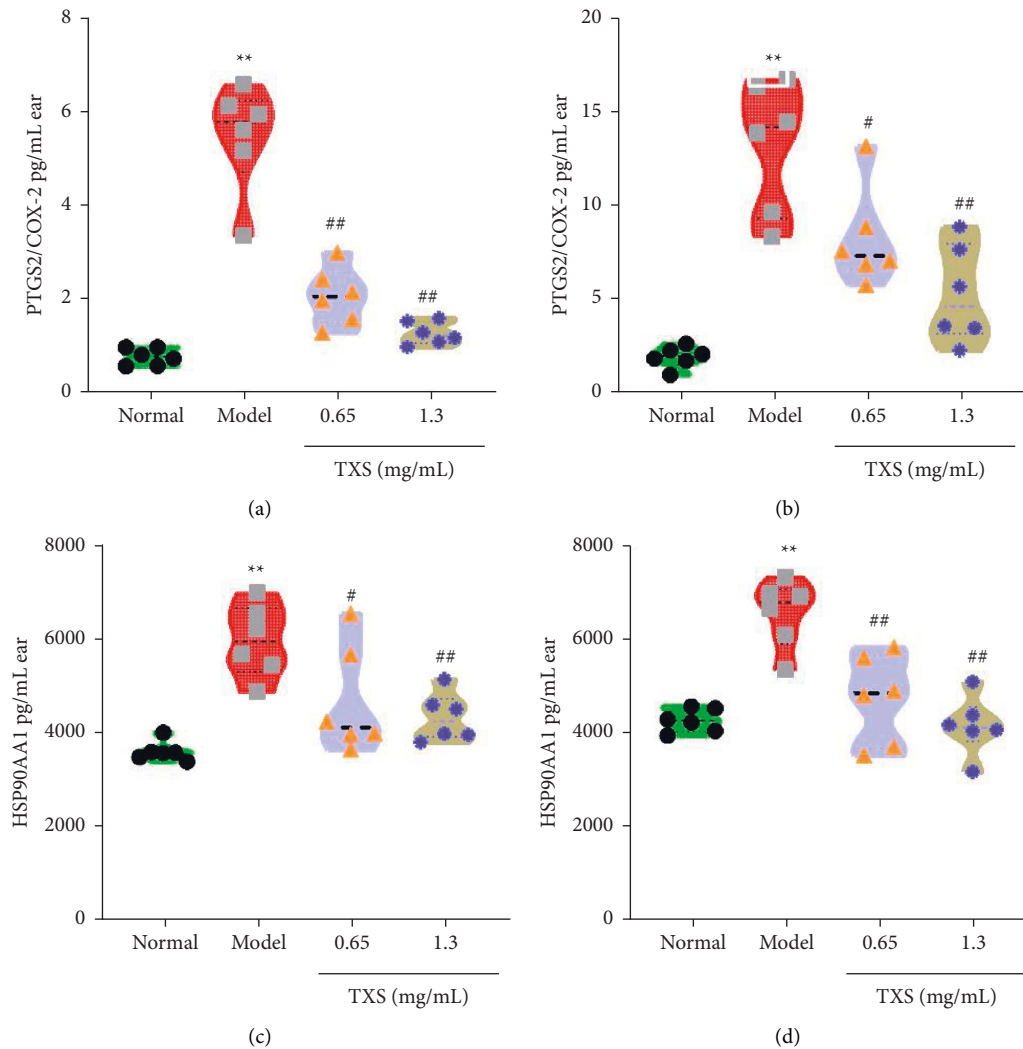
(a)

(b)

(c)

(d)

FIGURE 9: TXS alleviated AD via targeting PTGS2 and HSP90AA1. (a) The PTGS2 expression in ears was determined by ELISA. (b) The PTGS2 expression in skin was determined by ELISA. (c) HSP90AA1 in ears was calculated by ELISA. (d) HSP90AA1 in skin was calculated by ELISA. Values are expressed as mean ± SD ($n = 6$). * $P < 0.05$ and ** $P < 0.01$ compared with the normal group; ˆ$P < 0.05$ and ˆ$P < 0.01$ compared with the matrix group; #$P < 0.05$ and ##$P < 0.01$ compared with the DNFB model group.

ingredients from medicine and herbs [37, 38]. Therefore, we applied UPLC-Q-Exactive-Ms^E to analyze the information on compounds in herbal medicines of TXS. 65 components in TXS were identified, including alkaloids, phenols, flavonoids, and acids. Among them, various ingredients showed anti-inflammatory activity. Matrine, a quinolizidine alkaloid extracted from *Sophora flavescens*, has the capacity to effectively suppress experimental autoimmune enceph-alomyelitis and optic neuritis [39, 40]. Oxyberberine pre-vented lipopolysaccharide-induced acute lung injury and improved colitis [41, 42]. Epicatechin from *garden burnet*, epiberberine from *golden cypress*, and atractylenolide I from *Rhizoma atractylodis* showed anti-inflammatory activity [43–45]. Thus, we predict that TXS has an anti-inflammatory material basis.

The network pharmacology study as a major tool sys-tematically revealed the effects and mechanism of multi-component and multitarget system, such as traditional

Chinese medicine [46, 47]. Here, we researched the phar-macological mechanisms of TXS against atopic dermatitis through using the network analysis method. The ingredient-target gene network pharmacological analysis of TXS identified 52 ingredients and 137 target genes connected with AD. That means that one chemical component acted with an average of 9.03 targets, while one target was bound with an average of 3.43 compounds. The compound-target gene network of TXS revealed that (−)-epigallocatechin gallate (degree = 61, CC = 0.4797, BC = 0.3317), apigenin (degree = 41, CC = 0.4355, BC = 0.1750), and esculetin (degree = 34, CC = 0.4219, BC = 0.1296) were the major pharmacodynamic compositions of TXS according to the degree. Epigallocatechin gallate is a single ingredient from TCM and shows effective functions against AD due to the antioxidant and immunomodulatory effects [48]. Apigenin inhibits inflammatory cytokines (IL6, TNF-α, IL-5, and IL-13) production to decrease allergic responses in RBL-2H3

cells and repairs the physical barrier of the skin in HaCaT cell model [49]. Esculetin attenuates atopic skin inflammation by inhibiting IFN-γ, IL-13, IL-31, and IL-17 release via regulating nuclear factor-κB pathway [50]. Furthermore, in this network, the first 3 targets of degree values were PTGS2 (degree = 41, CC = 0.4846, BC = 0.1297), PTGS1 (degree = 27, CC = 0.3873, BC = 0.0358), and HSP90AA1 (degree = 21, CC = 0.3691, BC = 0.0224). Meanwhile, the three targets with higher BC and CC were recognized as critical targets of TXS for AD treatment. Thus, our results indicated that TXS as the complex system of herbal compounds displayed multipharmacological and superimposed effects.

Based on the enrichment results of KEGG, we determined that the effects of TSX against AD may be due to pathways like PI3K-Akt signaling pathway, MAPK signaling pathway, Th17 cell differentiation, and TLR signaling pathway. The mitogen-activated protein kinase (MAPK) pathway is responsible for inflammatory and immune response and is widely expressed in multiple tissues [51]. Previous study showed that *Solanum nigrum* Linne possessed anti-inflammatory effects in vitro through regulating MAPK/NF-κB pathway in HaCaT cell model [52]. It has been reported that inhibiting TLR signaling pathway was a critical approach for chronic allergic skin inflammation treatment [53]. *Artemisia argyi* Folium extract ameliorates DNCB-induced skin lesions in BALB/c mice via inhibiting PI3K/Akt pathway [54]. In this study, target genes enrichment was mainly associated with the biological processes including positive regulation of transcription from RNA polymerase II promoter, negative regulation of apoptotic process, inflammatory response, and positive regulation of transcription. Further, enriched MF ontologies were dominated through protein binding, enzyme binding, identical protein binding, and protein homodimerization activity. In addition, CC analysis displayed that cytoplasm was the largest constitution. Further, we found that TXS downregulated the expressions of PTGS2 and HSP90AA1. More importantly, the center target HSP90AA1 selected by the compound-target gene network was involved in the PI3K-Akt signaling pathway and PTGS2 was the major target for anti-inflammation.

5. Conclusions

In conclusion, our results revealed that TXS attenuated IL-4, IgE, and TNF-α levels in serum, increased thymus index, and decreased spleen index. TXS ameliorated behavioral changes and alleviated pathological changes of skin and ear in mice with the DNCB-induced atopic dermatitis. Additionally, TXS was mainly consisted of 65 chemical components. Among them, 52 components were closely associated with the effect of TXS against AD. TXS downregulated PTGS2 and HSP90AA1, which were associated with the PI3K-Akt signaling pathway. Our results revealed the effects, components, and pharmacological mechanism of TXS for AD, which provided scientific basis for clinical application.

Abbreviations

AD: Atopic dermatitis
TXS: Ta-Xi-San
DNCB: 2,4-Dinitrofluorobenzene
Th2: T helper 2
GO: Gene Ontology
IL: Interleukin
KEGG: Kyoto Encyclopedia of Gene and Genomics
LPS: Lipopolysaccharide
MAPK: Mitogen-activated protein kinase
NF: Nuclear factor
PPI: Protein-protein interaction
QTOF: Quadrupole-time of flight
TNF: Tumor necrosis factor
UPLC: Ultraperformance liquid chromatography
PTSG: Prostaglandin G/H synthase.

Data Availability

All the data used to support the findings of this study are submitted and are available in this published article.

Ethical Approval

All animal experiments were performed according to the protocol approved by Animal Ethics Committee and Institution Animal Care (license approval no.. SCXK (Shan) 2017-003).

Conflicts of Interest

The authors declare that they have no conflicts of interest.

Authors' Contributions

Wenbing Zhi conceived and designed the experiments. Wenbing Zhi wrote the manuscript and performed the studies. Yang Liu, Ye Li, and Li Chun performed the experiments. Hong Zhang and Yiding Zhao helped perform the analysis with constructive.

Acknowledgments

References

[1] T. Luger, M. Amagai, B. Dreno et al., "Atopic dermatitis: role of the skin barrier, environment, microbiome, and therapeutic agents," *Journal of Dermatological Science*, vol. 102, no. 3, pp. 142–157, 2021.

[2] B. Klasa and E. Cichocka-Jarosz, "Atopic dermatitis—current state of research on biological treatment," *Journal of mother and child*, vol. 24, no. 1, pp. 53–66, 2020.

[3] K. Hagenström, K. Sauer, N. Mohr et al., "Prevalence and medications of atopic dermatitis in Germany: claims data analysis," *Clinical Epidemiology*, vol. 13, pp. 593–602, 2021.

[4] Y. Ye, P. Zhao, L. Dou et al., "Dynamic trends in skin barrier function from birth to age 6 months and infantile atopic dermatitis: a Chinese prospective cohort study," *Clinical and Translational Allergy*, vol. 11, no. 5, 2021.

[5] K. Shetty and A. Sherje, "Nano intervention in topical delivery of corticosteroid for psoriasis and atopic dermatitis-a systematic review," *Journal of Materials Science: Materials in Medicine*, vol. 32, no. 8, 2021.

[6] J. Lee, J. Seok, I. Cho et al., "Topical application of celastrol alleviates atopic dermatitis symptoms mediated through the regulation of thymic stromal lymphopoietin and group 2 innate lymphoid cells," *Journal of Toxicology and Environmental Health Part A*, vol. 84, pp. 1–10, 2021.

[7] J. Meng, Y. Li, M. J. M Fischer, M. Steinhoff, W. Chen, and J. Wang, "Th2 modulation of transient receptor potential channels: an unmet therapeutic intervention for atopic dermatitis," *Frontiers in Immunology*, vol. 12, 2021.

[8] J. Bajgai, J. Xingyu, A. Fadriquela et al., "Effects of mineral complex material treatment on 2,4- dinitrochlorobenzene-induced atopic dermatitis like-skin lesions in mice model," *BMC complementary medicine and therapies*, vol. 21, no. 1, 2021.

[9] M. Zhang, T. Miura, S. Suzuki et al., "Vitamin K2 suppresses proliferation and inflammatory cytokine production in mitogen-activated lymphocytes of atopic dermatitis patients through the inhibition of mitogen-activated protein kinases," *Biological and Pharmaceutical Bulletin*, vol. 44, no. 1, pp. 7–17, 2021.

[10] M. Ota, T. Sasaki, T. Ebihara et al., "Filaggrin-gene mutation has minimal effect on the disease severity in the lesions of atopic dermatitis," *The Journal of Dermatology*, vol. 48, no. 11, pp. 1688–1699, 2021.

[11] H. Zeng, B. Zhao, X. Rui et al., "A tcm formula vyac ameliorates dncb-induced atopic dermatitis via blocking mast cell degranulation and suppressing nf-κb pathway," *Journal of Ethnopharmacol*, vol. 280, 2021.

[12] Z. F. Shi, T. B. Song, J. Xie, Y. Q. Yan, and Y. P. Du, "The traditional Chinese medicine and relevant treatment for the efficacy and safety of atopic dermatitis: a systematic review and meta-analysis of randomized controlled trials," *Evidence Based Complement Alternat Med*, vol. 2017, Article ID 6026434, 20 pages, 2017.

[13] O. Schachter, D. Perla, S. Greenberger, A. Barzilai, and S. Baum, "Traditional Chinese medicine in treatment of atopic dermatitis," *Harefuah*, vol. 155, no. 10, pp. 596–599, 2016.

[14] J. Choi, M. Y. Moon, G. Y. Han, M. S. Chang, D. Yang, and J. Cha, "Phellodendron amurense extract protects human keratinocytes from pm2.5-induced inflammation via PAR-2 signaling," *Biomolecules*, vol. 11, no. 1, 2020.

[15] X. He, J. Fang, L. Huang, J. Wang, and X. Huang, "Sophora flavescens Ait: traditional usage, phytochemistry and pharmacology of an important traditional Chinese medicine," *Journal of Ethnopharmacology*, vol. 172, pp. 10–29, 2015.

[16] M. Liu, M. Liao, C. Dai et al., "Sanguisorba officinalis L synergistically enhanced 5-fluorouracil cytotoxicity in colorectal cancer cells by promoting a reactive oxygen species-mediated, mitochondria-caspase-dependent apoptotic pathway," *Scientific Reports*, vol. 6, 2016.

[17] Y. Sun, G. Lenon, and A. Yang, "Phellodendri cortex: a phytochemical, pharmacological, and pharmacokinetic review," *Evidence-based Complementary and Alternative Medicine*, vol. 2019, Article ID 7621929, 45 pages, 2019.

[18] S. Park, D. S. Kim, S. Kang, and B. K. Shin, "Synergistic topical application of salt-processed Phellodendron amurense and Sanguisorba officinalis Linne alleviates atopic dermatitis symptoms by reducing levels of immunoglobulin E and pro-inflammatory cytokines in NC/Nga mice," *Molecular Medicine Reports*, vol. 12, no. 5, pp. 7657–7664, 2015.

[19] Y. Han, X. Zhang, Y. Kang et al., "Sophoraflavanone M, a prenylated flavonoid from Sophora flavescens Ait, suppresses pro-inflammatory mediators through both NF-κB and JNK/AP-1 signaling pathways in LPS-primed macrophages," *European Journal of Pharmacology*, vol. 907, 2021.

[20] Z. Zhang, X. Qin, Z. Wang et al., "Oxymatrine pretreatment protects H9c2 cardiomyocytes from hypoxia/reoxygenation injury by modulating the PI3K/Akt pathway," *Experimental and Therapeutic Medicine*, vol. 21, no. 6, 2021.

[21] C.-J. Gao, P.-J. Ding, L.-L. Yang et al., "Oxymatrine sensitizes the HaCaT cells to the IFN-γ pathway and downregulates MDC, ICAM-1, and SOCS1 by activating p38, JNK, and akt," *Inflammation*, vol. 41, no. 2, pp. 606–613, 2018.

[22] L. Cai, Z. Wei, X. Zhao, and Y. Li, X. Li and X. Jiang, Gallic acid mitigates LPS-induced inflammatory response via suppressing NF-κB signalling pathway in IPEC-J2 cells," *Journal of Animal Physiology and Animal Nutrition*, 2021.

[23] J.-l. Zhang, W.-m. Huang, and Q.-y. Zeng, "Atractylenolide I protects mice from lipopolysaccharide-induced acute lung injury," *European Journal of Pharmacology*, vol. 765, pp. 94–99, 2015.

[24] H. Lim, J. H. Lee, J. Kim, Y. S. Kim, and H. P. Kim, "Effects of the rhizomes of Atractylodes japonica and atractylenolide I on allergic response and experimental atopic dermatitis," *Archives of Pharmacal Research*, vol. 35, no. 11, pp. 2007–2012, 2012.

[25] M. Tsang, D. Jiao, B. C. Chan et al., "Anti-inflammatory activities of pentaherbs formula, berberine, gallic acid and chlorogenic acid in atopic dermatitis-like skin inflammation," *Molecules*, vol. 21, no. 4, 2016.

[26] M. Chu, M. Tsang, R. He, C. W. Lam, Z. B. Quan, and C. K. Wong, "The active compounds and therapeutic mechanisms of pentaherbs formula for oral and topical treatment of atopic dermatitis based on network pharmacology," *Plants (Basel, Switzerland)*, vol. 9, 2020.

[27] F. Hou, Y. Liu, Y. Cheng, N. Zhang, W. Yan, and F. Zhang, "Scutellaria baicalensisExploring the mechanism of georgi efficacy against oral squamous cell carcinoma based on network pharmacology and molecular docking analysis," *Evidence-Based Complementary And Alternative Medicine*, vol. 2021, Article ID 5597586, 2021.

[28] N. Wang, B. Yang, J. Zhang et al., "Metabolite profiling of traditional Chinese medicine XIAOPI formula: an integrated strategy based on UPLC-Q-Orbitrap MS combined with network pharmacology analysis," *Biomedicine and Pharmacotherapy*, vol. 121, 2020.

[29] C. Dunnick, M. Lehrer, H. Flaten et al., "Dermatology Tactile Learning Tool: development and student evaluation of an interactive 3-dimensional skin lesion model for medical student education," *Journal of the American Academy of Dermatology*, vol. 19, pp. S0190–S9622, 2019.

[30] H. Li, Z. Zhang, H. Zhang, Y. Guo, and Z. Yao, "Update on the pathogenesis and therapy of atopic dermatitis," *Clinical Reviews in Allergy and Immunology*, vol. 61, no. 3, pp. 324–338, 2021.

[31] E. Kim, S. Hong, J. M. Kim et al., "Effects of chloroform fraction of Fritillariae Thunbergii Bulbus on atopic symptoms in a DNCB-induced atopic dermatitis-like skin lesion model and in vitro models," *Journal of Ethnopharmacology*, vol. 281, 2021.

[32] T. Kim, Y. Kim, J. Jegal, B. G. Jo, H. S. Choi, and M. H. Yang, "Haplopine ameliorates 2,4-dinitrochlorobenzene-induced atopic dermatitis-like skin lesions in mice and TNF-α/IFN-γ-Induced inflammation in human keratinocyte," *Antioxidants*, vol. 10, no. 5, 2021.

[33] A. Bozek, M. Zajac, and M. Krupka, "Atopic dermatitis and psoriasis as overlapping syndromes," *Mediators of Inflammation*, vol. 2020, Article ID 7527859, 4 pages, 2020.

[34] L.-x. Fu, T. Chen, Z.-P. Guo, N. Cao, L.-W. Zhang, and P.-M. Zhou, "Enhanced serum interferon-lambda 1/interleukin-29 levels in patients with psoriasis vulgaris," *Anais Brasileiros de Dermatologia*, vol. 96, no. 4, pp. 416–421, 2021.

[35] L. Dong and C. Liu, "Effects of Loofah cylindrica extract on learning and memory ability, brain tissue morphology, and immune function of aging mice," *Open Life Sciences*, vol. 16, no. 1, pp. 399–407, 2021.

[36] M. Suttorp and C. Classen, "Splenomegaly in children and adolescents," *Frontiers in Pediatrics*, vol. 9, 2021.

[37] W. Zhang, K. Ren, S. Ren et al., "UPLC-Q-Exactive-MS analysis for hepatotoxicity components of Evodiae Fructus based on spectrum-toxicity relationship," *Journal of Chromatography B Analytical Technology Biomed Life Sci*, vol. 1176, 2021.

[38] X. Liu, J. Wang, B. Hu et al., "Qualitative distribution of endogenous sphingolipids in plasma of human and rodent species by UPLC-Q-Exactive-MS," *Journal of Chromatography BAnalytical Technology Biomed Life Sci*, vol. 1173, 2021.

[39] J. Kang, S. Liu, Y. Song et al., "Matrine treatment reduces retinal ganglion cell apoptosis in experimental optic neuritis," *Scientific Reports*, vol. 11, no. 1, 2021.

[40] Y. Chu, Y. Jing, X. Zhao et al., "Modulation of the HMGB1/TLR4/NF-κB signaling pathway in the CNS by matrine in experimental autoimmune encephalomyelitis," *Journal of Neuroimmunology*, vol. 352, 2021.

[41] R. Zhao, B. Wang, D. Wang, B. Wu, P. Ji, and D. Tan, "Oxyberberine prevented lipopolysaccharide-induced acute lung injury through inhibition of mitophagy," *Oxidative Medicine and Cellular Longevity*, vol. 2021, Article ID 6675264, 12 pages, 2021.

[42] C. Li, G. Ai, Y. Wang et al., "Oxyberberine, a novel gut microbiota-mediated metabolite of berberine, possesses superior anti-colitis effect: impact on intestinal epithelial barrier, gut microbiota profile and TLR4-MyD88-NF-κB pathway," *Pharmacological Research*, vol. 152, 2020.

[43] D. Milenkovic, K. Declerck, Y. Guttman et al., "(−)-Epicatechin metabolites promote vascular health through epigenetic reprogramming of endothelial-immune cell signaling and reversing systemic low-grade inflammation," *Biochemical Pharmacology*, vol. 173, 2020.

[44] L. Liu, J. Li, and Y. He, "Multifunctional epiberberine mediates multi-therapeutic effects," *Fitoterapia*, vol. 147, 2020.

[45] C. Wang, H. Duan, and L. He, "Inhibitory effect of atractylenolide I on angiogenesis in chronic inflammation in vivo and in vitro," *European Journal of Pharmacology*, vol. 612, pp. 143–152, 2009.

[46] X. Sun, J. Jiang, Y. Wang, and S. Liu, "Exploring the potential therapeutic effect of traditional Chinese medicine on coronavirus disease 2019 (COVID-19) through a combination of data mining and network pharmacology analysis," *European journal of integrative medicine*, vol. 40, Article ID 101242, 2020.

[47] Z. Li, F. Zhang, C. Fan et al., "Discovery of potential Q-marker of traditional Chinese medicine based on plant metabolomics and network pharmacology: periplocae Cortex as an example," *Phytomedicine*, vol. 85, Article ID 153535, 2021.

[48] Y.-H. Chiu, Y.-W. Wu, J.-I. Hung, and M.-C. Chen, "Epigallocatechin gallate/L-ascorbic acid-loaded poly-γ-glutamate microneedles with antioxidant, anti-inflammatory, and immunomodulatory effects for the treatment of atopic dermatitis," *Acta Biomaterialia*, vol. 130, pp. 223–233, 2021.

[49] C. Park, S. Min, H. Yu et al., "Effects of apigenin on RBL-2H3, RAW264.7, and HaCaT cells: anti-allergic, anti-inflammatory, and skin-protective activities," *International Journal of Molecular Sciences*, vol. 21, no. 13, 2020.

[50] N.-H. Jeong, E.-J. Yang, M. Jin et al., "Esculetin from Fraxinus rhynchophylla attenuates atopic skin inflammation by inhibiting the expression of inflammatory cytokines," *International Immunopharmacology*, vol. 59, pp. 209–216, 2018.

[51] X. Xiong, C. Huang, F. Wang et al., "Qingxue jiedu formulation ameliorated DNFB-induced atopic dermatitis by inhibiting STAT3/MAPK/NF-κB signaling pathways," *Journal of Ethnopharmacology*, vol. 270, Article ID 113773, 2021.

[52] S. Hong, B. Lee, J. H. Kim et al., "Solanum nigrum Linne improves DNCB-induced atopic dermatitis-like skin disease in BALB/c mice," *Molecular Medicine Reports*, vol. 22, no. 4, pp. 2878–2886, 2020.

[53] L. Tang, X. Li, Z. X Deng et al., "Conjugated linoleic acid attenuates 2,4-dinitrofluorobenzene-induced atopic dermatitis in mice through dual inhibition of COX-2/5-LOX and TLR4/NF-κB signaling," *The Journal of Nutritional Biochemistry*, vol. 81, Article ID 108379, 2020.

[54] H.-M. Han, S.-J. Kim, J.-S. Kim et al., "Ameliorative effects of Artemisia argyi Folium extract on 2,4-dinitrochlorobenzene-induced atopic dermatitis-like lesions in BALB/c mice," *Molecular Medicine Reports*, vol. 14, no. 4, pp. 3206–3214, 2016.